Effect of polymer–polymer interactions on the surface tension of colloid–polymer mixtures

A. Moncho-Jordá,[a] B. Rotenberg, and A. A. Louis[b]
Department of Chemistry, Lensfield Road, Cambridge CB2 1EW, United Kingdom

The density profile and surface tension for the interface of phase-separated colloid–polymer mixtures have been studied in the framework of the square gradient approximation for both ideal and interacting polymers in good solvent. The calculations show that in the presence of polymer–polymer excluded volume interactions the interfaces have lower widths and surface tensions compared to the case of ideal polymers. These results are a direct consequence of the shorter range and smaller depth of the depletion potential between colloidal particles induced by interacting polymers. © *2003 American Institute of Physics.* [DOI: 10.1063/1.1621613]

I. INTRODUCTION

Colloids are "soft" materials, readily deformable, with weak interfaces. This can be easily inferred from the "giant atom" picture of colloidal suspensions where, even though each colloid is made up of thousands of individual molecules, it is treated as a single particle interacting with an effective potential.[1,2] Since the effective interactions are roughly of the same shape as those of atomic fluids, an approximate corresponding states principle suggests that the reduced or dimensionless surface tensions should be similar. Near the fluid–fluid transition, the attractive interactions for both classes of fluids are typically of order $k_B T$, but the colloidal particles have radii R_c which can be 2 or 3 orders of magnitude larger than molecules. Thus, the surface tension, which scales as $\gamma \sim k_B T/R_c^2$, is expected to be four or more orders of magnitude lower than the values found for simpler atomic and molecular fluids. Similar approximate corresponding states arguments also explain why colloidal crystals are so easily deformable: their elastic constants, which scale as $k_B T/R_c^3$, are at least 6 orders of magnitude lower than those of simple atomic or molecular crystals. Colloids are indeed a form of "soft matter."

Surface tension plays an important role in the formation of interfaces, as well as in phase transition kinetics, nucleation, and spinodal decomposition.[3] Its indirect effects are therefore easily observable, but its low values make direct experimental measurements very difficult. Nevertheless, some recent experiments have made significant progress in measuring the fluid–fluid interface of colloid–polymer mixtures and its surface tension.[4,5] In these systems, adding nonadsorbing polymers induces attractive depletion pair potentials between the colloids,[6,7] which lead to the observed phase-transition between a colloid-rich ("liquid") and a colloid-poor ("gas") phase, separated by an interface. Because the experimental parameters can be easily tuned and controlled, colloid–polymer mixtures form an important model system for the study of phase transitions in soft matter.[8]

By applying theories similar to those used successfully for atomic and molecular fluids,[9] Vrij,[10] and Brader and Evans,[11] calculated the properties of this fluid–fluid interface for the case of ideal polymers, finding qualitative agreement with experiments. We have recently derived a depletion pair potential valid for interacting polymers,[12] which captures the dominant effects of polymer–polymer interactions on the phase diagrams.[13] This success suggests that the same potential can be used to calculate the properties of the fluid–fluid interface.

The main purpose of this paper is to investigate the effects of polymer–polymer interactions on the fluid–fluid interface of colloid–polymer mixtures. For that reason, we apply the same combination of thermodynamic perturbation theory[14] and square-gradient theory[9] that was used by Brader and Evans,[11] but with the new potential[12] instead of the Asakura–Oosawa (AO)[6,7] pair potential, valid only for ideal polymers. The differences between our new results, and those of Ref. 11, are then mainly due to the effect of polymer–polymer interactions.

The use of colloid–colloid depletion pair potentials describes one level of coarse graining. It is also possible to derive a more fundamental two-component picture based on polymer–polymer, polymer–colloid, and colloid–colloid pair potentials. A number of more recent investigations have used sophisticated two-component density functional theories (DFT) for the AO model[15] to uncover a host of interesting interfacial phenomena, including oscillatory density profiles at the fluid–fluid interface and a series of layering transitions at the fluid–hard-wall interface.[16] Computer simulations[17] have confirmed some of these results. At present, all these theories are only applicable to the AO model, and it is unfortunately not yet clear how to extend them to interacting polymers (see, however, Ref. 18). For that reason we restrict ourselves to the simplest square gradient approximation for the interfacial profiles.

Our paper is organized as follows: After briefly reviewing the nature of the depletion potentials and the equilibrium

[a]Electronic mail: amjm3@cam.ac.uk
[b]Electronic mail: aa120@cus.cam.ac.uk

phase diagrams in Sec. II, we describe the implementation of the square gradient approximation in Sec. III, and present our results for the interfacial tension and width in Sec. IV. Section V summarizes our conclusions.

II. ONE-COMPONENT EFFECTIVE DEPLETION INTERACTIONS

This section briefly describes the colloid–colloid effective depletion potentials for both ideal and interacting polymers. They are characterized by the polymer radius of gyration R_g, the colloid radius R_c, and the polymer number density ρ_p, or equivalently by the size-ratio $q = R_g/R_c$ and the reduced polymer density $\eta_p = \rho_p/\rho_p^*$, where $\rho_p^* = \frac{4}{3}\pi R_g^3$ is the so-called overlap density. In the ideal case, the depletion interaction between two isolated colloidal spheres at distance r is accurately approximated by a potential of the Asakura–Oosawa (AO) form

$$\beta V_{id}(r) = -\frac{4\pi}{3}\rho_p^r \sigma_{cp}^3 \left[1 - \frac{3}{4}\left(\frac{r}{\sigma_{cp}}\right) + \frac{1}{16}\left(\frac{r}{\sigma_{cp}}\right)^3 \right] \quad (1)$$

for $2R_c < r < 2(R_c + R_{AO}^{eff})$; $V_{id}(r) = 0$ for $r > 2(R_c + R_{AO}^{eff})$. Here, $\sigma_{cp} = (R_c + R_{AO}^{eff})$ and ρ_p^r is the polymer density in a reservoir in osmotic equilibrium with the full colloid–polymer mixture.[19] The range of this potential depends only on the polymer length and the depth is proportional to the polymer density. The effective Asakura–Oosawa parameter R_{AO}^{eff} is set by the requirement that the insertion free energy of one colloid is equal to that of ideal polymers;[20] it is given by[21]

$$R_{AO}^{eff} = R_c \left[\left(1 + \frac{6q}{\sqrt{\pi}} + 3q^2 \right)^{1/3} - 1 \right]. \quad (2)$$

For interacting polymers, we will use a recently proposed pair potential,[12] which accurately reproduces the depletion potentials obtained from direct computer simulations

$$V_s(r) = -\pi R_c \gamma_w(\rho_p^r) D_s(\rho_p^r) \left(1 - \frac{r - 2R_c}{D_s(\rho_p^r)} \right)^2 \quad (3)$$

for $2R_c < r < 2R_c + D_s$ and $V_s(r) = 0$ for $r > 2R_c + D_s$. Here $\gamma_w(\rho_p^r)$ is the surface tension of the polymer solution near a single wall[21] and $D_s(\rho_p^r)$ is the range of the potential, given by

$$D_s(\rho_p^r) = \sqrt{\pi} \frac{\gamma_w(\rho_p^r)}{\Pi(\rho_p^r)} \frac{R_{AO}^{eff}}{R_g}, \quad (4)$$

where Π is the osmotic pressure of the solution of interacting polymers, which is well understood.[22]

The range of V_{id} is independent of density, whereas the range of V_s shrinks with increasing density. Furthermore, for a given ρ_p^r and R_g, the well depth of V_{id} is greater than that of V_s, which implies that ideal polymers induce stronger depletion potentials than interacting polymers (see, e.g., Fig. 2 of Ref. 13 for some explicit examples).

The differences in pair potentials help explain why, for a given q, phase separation occurs at a larger value of η_p for interacting polymers than for ideal polymers,[23,24] a difference that grows with increasing q. Of course the pair-

potential approximation becomes increasingly unreliable at high q values, as many-body interactions become more important. However, we have recently shown[13] that calculations based on pair potentials alone remain remarkably accurate up to $q \sim 1$. In this paper we use the phase-diagrams calculated in Ref. 13, based on second order perturbation theory, as the basis for our calculations of the properties of the fluid–fluid interface. We make the implicit assumption that the effective Hamiltonian used for phase behavior is also appropriate for describing the interface. This follows from the fact that we are working at a contact chemical potential, so that the same effective potential holds across the density inhomogeneity occurring at the "free" interface (see Ref. 25).

III. INTERFACIAL PROPERTIES FROM THE SQUARE GRADIENT APPROXIMATION

Once phase separation occurs, there are two phases with well-defined colloidal bulk densities (ρ_c^G and ρ_c^L for the dilute and concentrated colloidal phases, respectively). Both phases are separated by a planar interface where the local density depends on the distance to the interface, $\rho_c(z)$. A well known way to treat the free-energy cost of making an interface is given by the square gradient approximation, where the free energy is expanded to lowest nontrivial order in a gradient expansion around the homogeneous fluid. The surface tension and the density profile are then obtained from the integral of the free energy across the interface[9,26–28]

$$\gamma = \int_{-\infty}^{\infty} \left[\Psi(\rho_c(z)) + \kappa \left(\frac{d\rho_c}{dz}\right)^2 \right] dz, \quad (5)$$

where $\Psi(\rho_c(z)) = \mathfrak{f}(\rho_c(z)) - \mu_c \rho_c(z) + P$. Here μ_c and P are the chemical potential and osmotic pressure of the colloids at coexistence and $\mathfrak{f}(\rho_c(z))$ is the Helmholtz free energy density of a hypothetical colloid fluid of density $\rho_c(z)$. The coefficient of the square gradient term, κ, describes the free-energy penalty for creating an interface. Minimizing this functional[10,27] leads to the following expressions for the density profile:

$$\left(\frac{d\rho_c}{dz}\right)^2 = \frac{\Psi}{\kappa} \quad (6)$$

and the surface tension

$$\gamma = 2 \int_{\rho_c^G}^{\rho_c^L} [\kappa \Psi]^{1/2} d\rho_c. \quad (7)$$

Requiring the functional in Eq. (5) to satisfy linear response relates the coefficient κ to properties of the direct correlation function $c(r)$ of the *homogeneous* fluid[9]

$$\kappa = \frac{\pi k_B T}{3} \int_0^{\infty} r^4 c(r, \rho_c) dr. \quad (8)$$

Note that all these variables depend implicitly on the polymer chemical potential (or equivalently the polymer reservoir density, ρ_p^r) of the corresponding coexistence point. Due to the factor r^4 in the integrand of expression (8), the value of κ is mainly determined by the behavior of $c(r)$ at large r, where it is well known that $c(r) \approx -\beta V(r)$. We therefore follow Ref. 11, and set $c(r, \rho_c)$ to be zero for
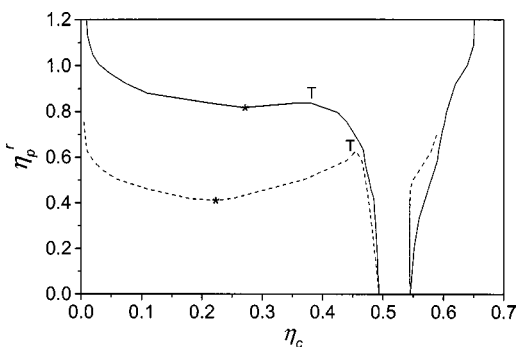
J. Chem. Phys., Vol. 119, No. 23, 15 December 2003

Surface tension of colloid–polymer mixtures   12669

FIG. 1. Phase diagrams of a colloid–polymer mixture for ideal (dashed lines) and interacting polymers (solid lines) compared for $q = R_g/R_c = 0.67$ (taken from Ref. 13). η_c is the colloidal packing fraction and η_p^r the reservoir polymer packing fraction. The binodal for interacting polymers is at a higher η_p than that of ideal polymers, because the latter are stronger depletants than the former.
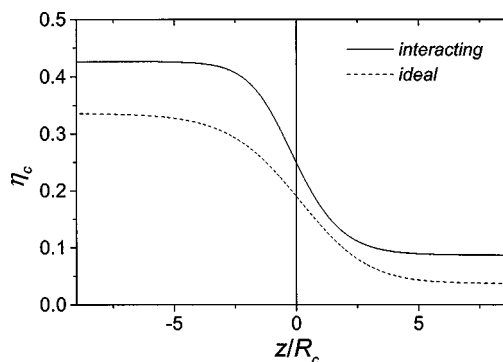

FIG. 2. Density profiles of the colloidal packing fraction for ideal and interacting polymers. In both cases, the size ratio is $q = 1.05$ and the relative polymer reservoir packing fraction from the critical point is ($\eta_p^r - \eta_p^{r,\text{crit}})/\eta_p^{r,\text{crit}} = 0.2$. Including polymer excluded volume interactions results in sharper interfaces.

$r < 2R_c$ and equal to $-\beta V(r)$ for $r > 2R_c$, where V is given by Eqs. (1) and (3) for ideal and interacting polymers, respectively. Hence Eq. (8) reduces to

$$\kappa \approx -\frac{\pi}{3} \int_{2R_c}^{\infty} V(r)r^4 \, dr. \qquad (9)$$

This approximation has the further advantage that it circumvents the conceptual difficulty of defining $c(r;\rho_c)$ in the coexistence region. Even though the approximation for $c(r)$ itself may not always be so reliable, we found that the values of κ still compare well with more sophisticated calculations of $c(r)$, because this simple model interpolates between the values at the two coexistence points. Similar conclusions were reached in a paper studying Lennard-Jones systems,[29] where the Percus–Yevick approximation for the low and high density fluid phases was combined with a lever rule to obtain $c(r)$ in the coexistence region.

IV. RESULTS AND DISCUSSION

A. Phase behavior and interfacial properties

In our earlier work,[13] the free energy densities for the effective one-component system, $f(\rho_c)$, were calculated for various q ratios by second order perturbation theory using the Barker–Henderson formulation.[30] The phase diagrams were determined by the common tangent construction. The resulting coexistence curves for ideal and interacting polymers are plotted in Fig. 1, for size ratio $q = 0.67$, as a function of the colloid packing fraction $\eta_c = 4\pi\rho_c R_c^3/3$ and polymer reservoir packing fraction $\eta_p^r = 4\pi\rho_p^r R_g^3/3$. The fluid–fluid coexistence lines are at higher values of polymer packing fraction for interacting polymers, which implies that polymer excluded volume effects reduce the global attraction between colloidal particles. But not only is the position of the binodal different, so is its shape. In particular, the binodal is flatter and the separation between the critical and triple points is smaller for interacting polymers. This effect is not merely an artifact of the pair-potential approximation. The qualitative difference in shape is also observed when comparing two-component simulations of ideal and interacting polymer models.[24] Although we only show results for one

size ratio in Fig. 1, the differences become more pronounced for increasing q,[13,24] and are finally quite dramatic in the so-called protein limit where $q \gg 1$.[31]

It should be noted that, at least within our perturbation theory treatment, the gas–liquid binodal obtained for interacting polymers at $q = 0.34$ is metastable with respect to the fluid–solid coexistence. This is not, however, an obstacle to the calculation of surface tensions. Furthermore, in many experimental systems the fluid–solid nucleation rates are very low, allowing the observation of metastable fluid–fluid phase separation.

The free energy densities from perturbation theory were used in Eqs. (6) and (7) to calculate first the density profiles and then the surface tensions for the coexistence points along the fluid–fluid binodal. Two typical density profiles corresponding to ideal and interacting polymers are shown in Fig. 2 for $q = 1.05$ and $\Delta\eta_p^r = (\eta_p^r - \eta_p^{r,\text{crit}})/\eta_p^{r,\text{crit}} = 0.2$. All profiles obtained using the square gradient theory share approximately the same shape, i.e., a smooth monotonic curve which goes from the dense to the dilute colloidal phase. Comparison between both curves shows that the difference between the colloidal packing fractions in the two phases is larger for interacting polymers (a consequence of the flatter binodals), whereas the interfacial thickness is smaller.

The interfacial profiles can be characterized by their width. The 10–90 width of the interface (W), defined as the distance along the interface over which the colloidal density varies from $(\eta_c^G + 0.1(\eta_c^L - \eta_c^G))$ to $(\eta_c^G + 0.9(\eta_c^L - \eta_c^G))$, is plotted in Fig. 3 with respect to the deviation of the polymer reservoir packing fraction from the critical point. As expected, the interface is very diffuse near the critical point, and becomes sharper upon approaching the triple point. The interfacial widths increase with increasing q, reflecting the longer ranged attractions. For a given value of q, the widths are consistently lower for interacting polymers than for ideal polymers.

The resulting dimensionless surface tensions ($\gamma R_c^2/k_B T$) are shown in Fig. 4 versus the difference in colloidal packing fractions between both phases for three different size ratios, $q = 0.34$, 0.67, and 1.05. For both ideal and interacting polymers, the surface tension vanishes at the critical point, and
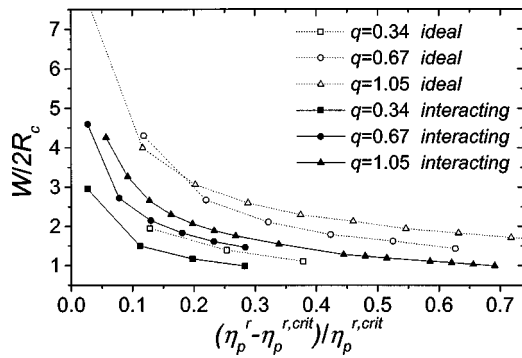
FIG. 3. The 10–90 width of the interface for ideal (white symbols) and interacting polymers (black symbols) vs the deviation of the polymer reservoir packing fraction from the critical point, for $q=0.34$, 0.67, and 1.05. Including polymer excluded volume interactions reduces the width of the interface.

FIG. 5. Effective colloid–colloid depletion pair potential induced by interacting (solid line) and ideal polymers (dashed line) for $q=0.67$ at their respective critical points, as a function of the distance between the particle surfaces $x=r-2R_c$. Inset: ratio between the κ parameter for interacting and ideal polymers at the critical point vs the size ratio q.

increases with $\Delta\eta_c=\eta_c^L-\eta_c^G$ as expected. These reduced values are of the same order as those found for simple liquids.[9] Their absolute values depend only on R_c; typical colloid sizes result in values of γ near the triple point on the order of μN/m which is much smaller than the values of 10–100 mN/m found for simple fluids. For a given $\Delta\eta_c$, the surface tension increases with q. Moreover, for a given q the ideal polymer surface tension is always significantly larger than that of interacting polymers.

In view of the mean field nature of the present theory, the critical exponents are obviously classical, i.e., $\gamma\propto\Delta\eta_c^3$ and $W\propto\Delta\eta_c^{-1}$. However, the prefactors are expected to be different for ideal and interacting polymer depletants. These prefactors are determined in the following section. For ideal polymers similar scaling laws with the reservoir density ρ_p^r can also be derived, by exploiting the analogy with inverse temperature. For example,[11] $W\propto(\Delta\eta_p^r)^{-1/2}$. However, for interacting polymers such a simple scaling with ρ_p^r does not follow, because the effective well-depths (i.e., the inverse "temperatures") do not scale in a simple way with this variable.

B. Connection to the form of the depletion potential

The results of the preceding section show that both the 10–90 width, and the interfacial tension, are lower in the
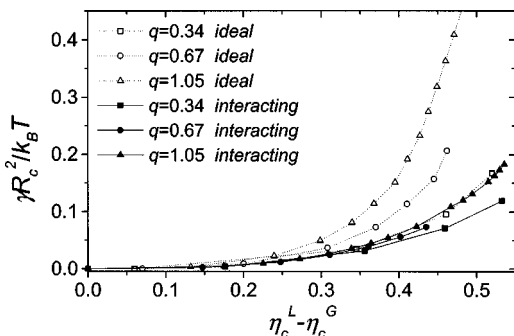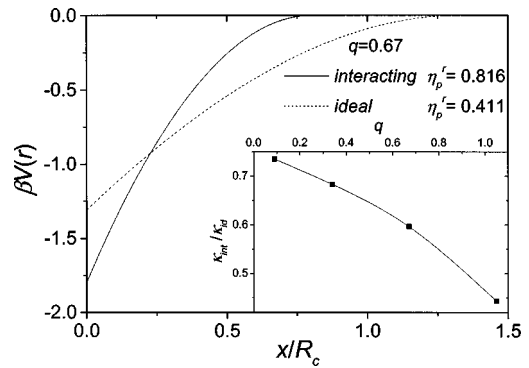

FIG. 4. Dimensionless surface tensions for ideal (white symbols) and interacting polymers (black symbols) as a function of $\eta_c^L-\eta_c^G$ for $q=0.34$, 0.67, and 1.05.

case of interacting polymers. In this section, we will attempt to rationalize these differences on the basis of the effective pair potentials.

Close to the critical point, $\Psi(\eta_c)$ can be approximated as the product of two quadratic potential wells centered around the coexistence points[3]

$$\Psi^*(\eta_c)\approx\frac{C}{2}(\eta_c-\eta_c^G)^2(\eta_c-\eta_c^L)^2,\tag{10}$$

where $\Psi^*=(4\pi R_c^3/3)\beta\Psi$ is dimensionless and $C=(1/12)d^4\Psi^*/d\eta_c^4$, calculated at the critical point. If we assume that κ is independent of ρ_c, as we did in the preceding section, then inserting Eq. (10) into Eq. (7) yields the following expression for the reduced surface tension:

$$\gamma^*=\frac{R_c^2\gamma}{k_BT}\approx0.0275\sqrt{C}\sqrt{\kappa^*(\eta_p^r)}(\eta_c^L-\eta_c^G)^3,\tag{11}$$

where $\kappa^*=\beta\kappa/R_c^5$. The dependence of κ^* on the polymer reservoir packing fraction is indicated explicitly to remind us that it is not a constant parameter but rather increases as we move away from the critical point since it depends on η_p^r through $V(r)$. The same arguments lead to[3]

$$W\sim\sqrt{\frac{\kappa^*(\eta_p^r)}{C}}(\eta_c^L-\eta_c^G)^{-1}.\tag{12}$$

The values of W and γ^* are determined by the parameters κ^* and C. Equation (9) directly relates κ to the depletion potential, whereas C is given by the shape of the free energy inside the van der Waals loop. Understanding how the depletion potentials govern the interfacial behavior now reduces to explaining how these two parameters depend on the potentials.

Figure 5 compares the depletion pair potential for ideal and interacting polymers at their corresponding critical points when $q=0.67$. Even though the depletion potential for interacting polymers has a larger depth at contact, its range is significantly shortened by the polymer excluded volume interactions.[12] The integrand in Eq. (9), which determines κ, multiplies the potential by r^4, giving extra weight to the longer ranged parts of the potentials. Thus the ratio of κ_{int}^*

[calculated with Eq. (3)] to κ_{id}^* [calculated with the potential of Eq. (1)], is always less than 1, and decreases with increasing q, as shown in the inset of Fig. 5. It has been recently shown that the reduced second virial coefficient, which is proportional to the integral of $r^2(\exp[-\beta V(r)]-1)$, is very similar at the critical point for a wide class of attractive potentials.[32] This observation remains true for the two depletion potentials, giving further support to our argument that it is the large factor r^4 in the integrand for κ which is responsible for the differences between κ_{id}^* and κ_{int}^*.

The value of the other parameter, C, is not as easy to link directly to the pair potential. Nevertheless, it can be determined numerically from our previous calculations of the surface tension. It turns out not to depend strongly on q. We find $C=85.8\pm0.5$ for ideal and $C=76.0\pm0.3$ for interacting polymers, the small difference perhaps reflecting the fact that the free energy loop is slightly flatter for interacting polymers.

Compared to the large changes in the surface tension, the values of C are quite similar, so that differences in the γ's, which scale as $\gamma\sim\sqrt{\kappa^*C}$, arise mainly from κ. Since κ increases with the range of the potential, i.e., with q, this explains why, for a given type of depletant, the surface tension grows with q. It further shows how the main differences in γ^* between ideal and interacting polymers are linked to the reduction of the depletion potential range induced by polymer–polymer interactions. Since this effect becomes more important for increasing q, we expect the differences between the surface tensions induced by ideal and interacting polymers to grow with q as well, and to become more pronounced in the protein limit,[31] as was recently pointed out by Sear.[33,34]

The interfacial width scales as $W\sim\sqrt{\kappa^*/C}$. Again, differences in W are dominated by κ. Thus, the net effect of adding polymer–polymer interactions is to decrease the interfacial width.

These results show that the decrease of the range in the depletion potential, caused by the polymer interactions, plays the dominant role in determining the differences in the interfacial properties between the two types of depletants. The change in the depth of the potential is only a secondary effect.

In all the arguments above it should be kept in mind that our double symmetric parabola approximation of Eq. (11) is only valid close to the critical point. For coexistence points far from it, the bulk correlation length [defined as $\xi_b=(2\kappa/(d\mu_c(\rho_b)/d\rho_b))^{1/2}$, where ρ_b is the colloidal density in the bulk phase] does differ between the two phases, implying that the decay of the profile tails is different between the liquid and the gas colloidal phase.[29] Strictly speaking, more sophisticated theories are needed in order to describe the interfacial properties near the triple point. DFT theories of the fluid–fluid interface in the two-component AO model suggest that for ideal polymers, the square gradient approximation underestimates the values of the interfacial tension,[16] and that it misses more subtle effects like oscillatory density profiles. Part of the difference comes from using more accurate DFT's, but some also arises from the fact that the two-component DFT yields different phase-diagrams than the ef-

fective one-component description.[15] In particular, the two-component theories yield a larger distance between the critical point and the triple point,[17,20] which may have an important qualitative and quantitative effect on the interfacial behavior. While it would clearly be desirable to have a two-component theory of similar accuracy for interacting polymers, this is not available at present. However, it is possible to use more sophisticated DFT[35] approaches to study the one-component interacting polymer system, a direction which we are now pursuing. In fact, we have already performed preliminary calculations using an accurate DFT for the HS part, and with the interaction of Eq. (3) treated as a perturbation.[36] The results for surface tensions and interfacial widths are slightly higher than those from the present treatment, but the trends are very similar. This suggests that our use of the square gradient theory, coupled with our rather simple approximation for $c(r)$, as used in Eq. (9), is quite reliable.

In the longer term, it would be interesting to develop some approximate density functional for interacting polymers using a two-component representation, perhaps along the lines of Ref. 18, in order to obtain accurate predictions of the interfacial properties of free fluid–fluid interfaces, adsorption and wetting behavior at hard walls and even surface tensions and density profiles of fluid–solid interfaces.

Although the actual values of the surface tensions found within the square gradient theory may only be accurate to about a factor of 2, the differences between ideal and interacting polymers are fairly large, and follow from a simple physical explanation which seems robust. We therefore do not expect more sophisticated theories to reverse the trends discussed in this paper. On the other hand, whether or not the more subtle interfacial phenomena found for the two-component AO model[16,17] will be even qualitatively similar for interacting polymers remains to be seen. For example, in the latter case the differences between the triple and critical points are less pronounced, which may lead to less well-defined oscillations in the density profiles. Clearly more work remains to be done.

The square gradient theory does not include the effects of capillary fluctuations,[9] but these are not expected to be large, as shown in Ref. 11. We can therefore make comparisons with experiments. Full two-component AO model calculations within DFT[16] lead to values of the surface tension that are close to those of recent experiments.[4] However, our results suggest that including polymer–polymer interactions will lower the value of the surface tension, leading to less agreement.

V. CONCLUSION

We have used thermodynamic perturbation theory and the square-gradient approximation to calculate the properties of the fluid–fluid interface for mixtures of colloids and interacting polymers within an effective one-component representation. We find significant differences compared to the case of ideal polymers. The main effect of polymer–polymer excluded volume interactions is to reduce the value of the interfacial tension γ and the interface width W. This effect becomes more pronounced as the size-ratio q increases. It

can be rationalized by the differences in depletion potentials: at the critical point, the range for the interacting polymer case is significantly less than for the ideal case. This has a pronounced effect on the square gradient prefactor κ, and helps explain the differences between the two types of depletants.

ACKNOWLEDGMENTS

[1] D. Frenkel, in *Soft and Fragile Matter*, edited by M. E. Cates and M. R. Evans (Institute of Physics, London, 2000).

[2] C. N. Likos, Phys. Rep. **348**, 267 (2001).

[3] J. L. Barrat and J. P. Hansen, *Basic Concepts for Simple and Complex Liquids* (Cambridge University Press, Cambridge, 2003).

[4] E. H. A. de Hoog and H. N. W. Lekkerkerker, J. Phys. Chem. B **103**, 5274 (1999).

[5] E. H. A. de Hoog, H. N. W. Lekkerkerker, J. Schulz, and G. H. Findenegg, J. Phys. Chem. B **103**, 10657 (1999); D. G. A. L. Aarts, J. van der Wiel, and H. N. W. Lekkerkerker, J. Phys.: Condens. Matter. **15**, S245 (2003).

[6] S. Asakura and F. Oosawa, J. Chem. Phys. **22**, 1255 (1954).

[7] S. Asakura and F. Oosawa, J. Polym. Sci., Polym. Symp. **34**, 183 (1958); A. Vrij, Pure Appl. Chem. **48**, 471 (1976).

[8] W. C. K. Poon, J. Phys.: Condens. Matter **14**, R859 (2002).

[9] J. S. Rowlinson and B. Widom, *Molecular Theory of Capillarity* (Clarendon, Oxford, 1982).

[10] A. Vrij, Physica A **235**, 120 (1997).

[11] J. M. Brader and R. Evans, Europhys. Lett. **49**, 678 (2000).

[12] A. A. Louis, P. G. Bolhuis, E. J. Meijer, and J. P. Hansen, J. Chem. Phys. **117**, 1893 (2002).

[13] B. Rotenberg, J. Dzubiella, J.-P. Hansen, and A. A. Louis, Mol. Phys. http://arxiv.org/abs/cond-mat/0305533 (to be published).

[14] J.-P. Hansen and I. R. McDonald, *Theory of Simple Liquids*, 2nd ed. (Academic, London, 1986).

[15] M. Schmidt, H. Löwen, J. M. Brader, and R. Evans, Phys. Rev. Lett. **85**, 1934 (2000).

[16] J. M. Brader, R. Evans, M. Schmidt, and H. Löwen, J. Phys.: Condens. Matter **14**, L1 (2002).

[17] M. Dijkstra and R. van Roij, Phys. Rev. Lett. **89**, 208303 (2002).

[18] M. Schmidt, A. R. Denton, and J. M. Brader, J. Chem. Phys. **118**, 1541 (2003).

[19] H. N. W. Lekkerkerker, W. C. K. Poon, P. N. Pusey, A. Stroobants, and P. B. Warren, Europhys. Lett. **20**, 559 (1992).

[20] E. J. Meijer and D. Frenkel, Phys. Rev. Lett. **67**, 1110 (1991); J. Chem. Phys. **100**, 6873 (1994).

[21] A. A. Louis, P. G. Bolhuis, J. P. Hansen, and E. J. Meijer, J. Chem. Phys. **116**, 10547 (2002).

[22] L. Shäfer, *Excluded Volume Effects in Polymer Solutions* (Springer-Verlag, Berlin, 1999).

[23] S. Ramakrishnan, M. Fuchs, K. S. Schweizer, and C. F. Zukoski, J. Chem. Phys. **116**, 2201 (2002).

[24] P. G. Bolhuis, A. A. Louis, and J.-P. Hansen, Phys. Rev. Lett. **89**, 128302 (2002).

[25] J. M. Brader, M. Dijkstra, and R. Evans, Phys. Rev. E **63**, 041405 (2001).

[26] J. W. Cahn and J. E. Hilliard, J. Chem. Phys. **28**, 258 (1958).

[27] R. Evans, Adv. Phys. **28**, 143 (1979).

[28] R. Evans, *Fundamentals of Inhomogeneous Fluids* (Dekker, New York, 1992).

[29] B. Q. Lu, R. Evans, and M. M. Telo da Gama, Mol. Phys. **55**, 1319 (1985).

[30] J. A. Barker and D. J. Henderson, J. Chem. Phys. **47**, 2856 (1967).

[31] P. G. Bolhuis, E. J. Meijer, and A. A. Louis, Phys. Rev. Lett. **90**, 068304 (2003).

[32] G. A. Vliegenthart and H. N. W. Lekkerkerker, J. Chem. Phys. **112**, 5364 (2000).

[33] R. P. Sear, Phys. Rev. E **65**, 062401 (2002).

[34] R. P. Sear, J. Chem. Phys. **116**, 2922 (2002).

[35] J. Winkelmann, J. Phys.: Condens. Matter **13**, 4739 (2001).

[36] A. Moncho-Jorda, J.-P. Hansen, and A. A. Louis (unpublished).